Strain sensor using stress-magnetoresistance effect of Ni–Fe/Mn–Ir exchange-coupled magnetic film

M. Sonehara,[a] T. Shinohara, T. Sato, K. Yamasawa, and Y. Miura
Spin Device Technology Center, Shinshu University, 4-17-1 Wakasato, Nagano 380-8553, Japan

(Presented 21 January 2010; received 4 November 2009; accepted 23 November 2009; published online 6 May 2010)

A strain sensor using a stress-magnetoresistance effect of a Ni–Fe/Mn–Ir exchange-coupled magnetic film was fabricated and evaluated. The stress magnetoresistance is used in the inverse magnetostrictive effect and the magnetoresistance effect in the magnetic film since an external stress is changed into an electric resistance in it. A compressive stress was measured by the strain sensor with a Mn–Ir (10 nm)/Ni–Fe (50 nm)/Ru (1 nm) exchange-coupled film. The change in resistivity $\Delta\rho/\rho$ is proportional to the applied compressive stress σ for $\sigma \leqq 50$ MPa in the strain sensor. When increasing Ni–Fe layer thickness in the strain sensor, a gauge factor increased. © *2010 American Institute of Physics*. [doi:10.1063/1.3362902]

I. INTRODUCTION

The strain sensor using stress-magnetoresistance effect is possible to detect microstress. Such the sensor exhibits sensitivity performance superior to a metallic wire electrical-resistance strain gauge. The stress-magnetoresistance[1] (stress-MR) used in the inverse magnetostrictive[2] and MR effects[3] in the magnetic film due to its capability to change it electric resistance proportionally to an applied stress is changed into an electric resistance in it. When an angle of an easy axis in the magnetic film, a direction of current, and a direction of applied stress was 45°, linear strain sensing was obtained by the calculated result for the stress-MR effect.[4]

The authors proposed a strain sensor with a method of turning the easy axis to 45° using a pinning field for a ferro-/antiferromagnetic exchange-coupled film. In addition, the sensitivity of the strain sensor can be controlled by changing a ferromagnetic layer thickness t_F. The fact that the exchange bias field H_{ex} and the static susceptibility χ_{h0} in the hard axis of the exchange-coupled film are described by following equations:[5]

$$H_{ex} = J_{ex}/M_s t_F, \tag{1}$$

$$\chi_{h0} = M_s/\mu_0(H_k + H_{ex}), \tag{2}$$

where J_{ex} is the exchange energy, M_s is the saturation magnetization, and H_k is the uniaxial anisotropy magnetic field in the ferromagnetic layer. Since static susceptibility χ_{h0} can be changed easily by the ferromagnetic layer thickness t_F. $Ni_{87}Fe_{13}$ (at. %) with a high MR ratio was selected for the ferromagnetic film. $Mn_{80}Ir_{20}$ (at. %) was selected for the antiferromagnetic film.[6] As already reported previously,[7] one directional anisotropy dispersion of the ferromagnetic film became smaller when a 1 nm Ru film was used as an ultrathin underlayer for the ferromagnetic film so that an improvement of magnetic properties was observed. This paper describes a development and characterizations of a strain sensor using stress-MR effect of Mn–Ir/Ni–Fe/Ru exchange-coupled magnetic film.

II. FABRICATION

Figure 1 shows schematic and dimensions of the strain sensor using stress-MR effect. The strain sensor was fabricated by following process.

First, a photoresist 2×5 mm^2 pattern was formed on a glass substrate (30×30 mm^2, 160 μm thick), then Mn–Ir (10 nm)/Ni–Fe (t_F nm)/Ru (1 nm) exchange-coupled magnetic films were fabricated by rf magnetron sputtering (t_F =30, 50, and 70 nm). The films were deposited under dc magnetic field of 75 Oe in parallel with the film plane. The sputtering conditions for Ru, Ni–Fe, and Mn–Ir are shown in Table I. Moreover then the photoresist was removed by lift-off method.

Second, a photoresist pattern was formed, as shown in Fig. 1, then Cu (200 nm)/Cr (50 nm) for the electrodes was fabricated by dc magnetron sputtering, and then the photoresist was removed by lift-off method.

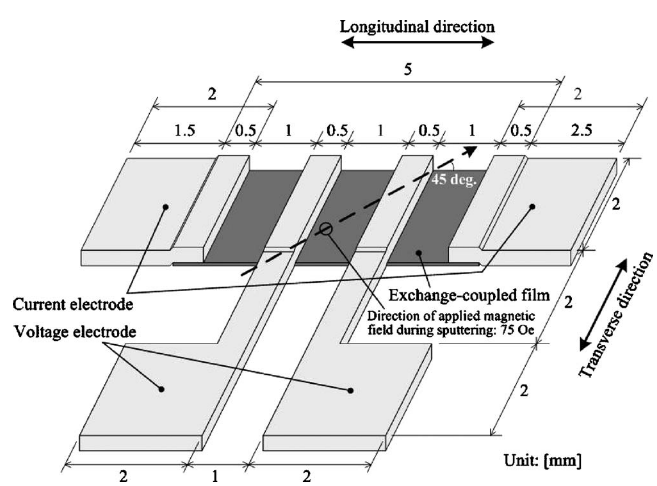

FIG. 1. Schematic and dimensions of the strain sensor.

[a]Electronic mail: makoto@shinshu-u.ac.jp.

TABLE I. Sputtering conditions of Ru, Ni–Fe, and Mn–Ir films.

	Ru	Ni–Fe	Mn–Ir
3 in. target	Ru	$Ni_{87}Fe_{13}$ (at. %)	$Mn_{80}Ir_{20}$ (at. %)
Base pressure		$<9\times10^{-5}$ Pa	
Ar pressure	0.7 Pa	0.6 Pa	0.9 Pa
rf power	100 W	300 W	100 W
Remarks	⋯	Substrate rotation 15 rpm	⋯

III. MEASUREMENT

The magnetization curves of the Mn–Ir/Ni–Fe exchange-coupled magnetic films are evaluated using a vibrating sample magnetometer (Riken Denshi, BHV-55). A change in a resistivity $\Delta\rho/\rho$ in the sensor with the MR was measured by a four terminal method using a digital multi meter (ADVANTEST, R6971).

The fabricated strain sensor was pasted by an adhesive for the strain gauge (Kyowa dengyo, CC-33A) on a center of SUS304 nonmagnetic cuboid ($20\times20\times40$ mm^3). An autograph (Shimadzu, AG-100KNGH) was used to apply a compressive stress to the longitudinal direction in Fig. 1. Finally a change in the resistivity $\Delta\rho/\rho$ in the sensor with the applied compressive stress was measured by the digital multimeter.

IV. RESULTS AND DISCUSSION

A. Magnetization curves in exchange-coupled film

Figure 2 shows the typical magnetization curves measured for the Mn–Ir (10 nm)/Ni–Fe (50 nm)/Ru (1 nm) exchange-coupled film. The saturation field H_s, as shown in Fig. 2, was defined by using a tangential line at zero field in the hard axis magnetization curve.

Figure 3 shows a relation between exchange bias field H_{ex}, saturation field H_s, and Ni–Fe layer thickness t_F, which were estimated from easy and hard axis magnetization curves. In Fig. 3, exchange bias field H_{ex} is nearly inversely proportional to the Ni–Fe layer thickness t_F. This result agrees with Eq. (1). The exchange energy J_{ex} of the Mn–Ir/Ni–Fe interface was estimated to be 0.043 erg/cm^2, which was about 30% of the Mn–Ir/Fe–Si interface.[8]

ΔH defined as a difference between saturation field H_s and exchange bias field H_{ex} was estimated to be about 3.6 Oe

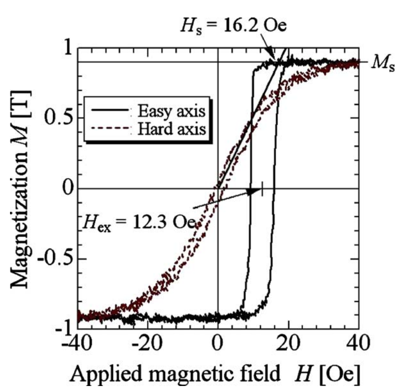

FIG. 2. (Color online) Typical magnetization curves measured for the Mn–Ir (10 nm)/Ni–Fe (50 nm)/Ru (1 nm) exchange-coupled film.

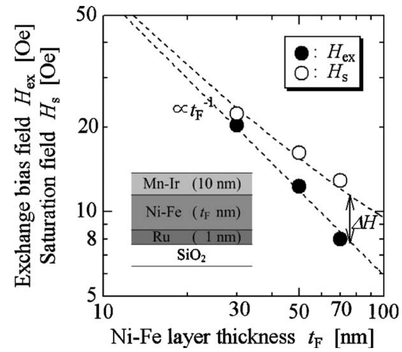

FIG. 3. Relation between exchange bias field H_{ex}, saturation field H_s, and Ni–Fe layer thickness t_F in the Mn–Ir (10 nm)/Ni–Fe (t_F nm)/Ru (1 nm) exchange-coupled film.

from Fig. 3, which is close to the intrinsic uniaxial anisotropy field H_k (~3.5 Oe) of the single Ni–Fe film.[4]

Table II shows the predicted static hard axis susceptibilities χ_{h0} for three kinds of the films, which were estimated by using Eq. (2) and $H_s=H_k+H_{ex}$. Static susceptibility χ_{h0} can be controlled by changing Ni–Fe layer thickness t_F only.

B. MR effect

Figure 4 shows the typical relation between applied magnetic field H and the change in resistivity $\Delta\rho/\rho$ measured for the strain sensor with (a) the Mn–Ir (10 nm)/Ni–Fe (50 nm)/Ru (1 nm) exchange-coupled film and (b) the Ni–Fe (100 nm)/Ru (1 nm) magnetic film. The $H\|I$ means that a direction of the applied magnetic field H corresponded to the longitudinal direction in the strain sensor, as shown Fig. 4. On the other hand, the $H\perp I$ means that H corresponded to the transverse direction in the strain sensor. When the angle θ of the easy axis in the magnetic film and longitudinal direction was 45°, an absolute value of $\Delta\rho/\rho$ in the $H\|I$ is equal to that in the $H\perp I$.[4]

In Fig. 4(b), the absolute value of $\Delta\rho/\rho$ in the $H\|I$ is not consistent with that in the $H\perp I$, and angle θ was estimated to be about 75°.[4] On the other hand, an absolute value of $\Delta\rho/\rho$ in the $H\|I$ is approximately equal to that in the $H\perp I$, as shown Fig. 4(a). Moreover angle θ was estimated to be about 46° because of pinning field for the exchange-coupled film.

C. Stress-magnetoresistance effect

Figure 5 shows relation between change in resistivity $\Delta\rho/\rho$ for the stress-MR effect, strain $\Delta l/l$, and applied compressive stress σ in the strain sensor with Mn–Ir (10 nm)/Ni–Fe (50 nm)/Ru (1 nm) exchange-coupled film. In Fig. 5,

TABLE II. Predicted static susceptibility χ_{h0} in the Mn–Ir (10 nm)/Ni–Fe (t_F nm)/Ru (1 nm) exchange-coupled film.

t_F (nm)	M_s (T)	H_s (Oe)	χ_{h0}
30	0.9	22.3	404
50	0.9	16.2	556
70	0.9	12.9	698

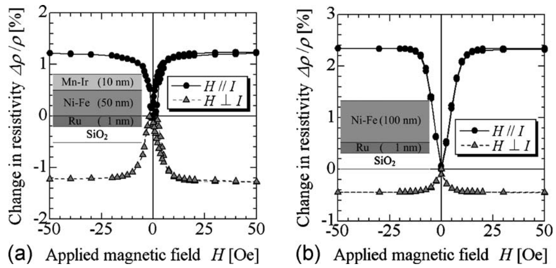

FIG. 4. Typical relation between applied magnetic field H and change in resistivity $\Delta\rho/\rho$ measured for the strain sensor with (a) the Mn–Ir (10 nm)/Ni–Fe (50 nm)/Ru (1 nm) exchange-coupled film and (b) the Ni–Fe (100 nm)/Ru (1 nm) magnetic film.

the change in resistivity $\Delta\rho/\rho$ is proportional to the applied compressive stress σ for $\sigma \leqq 50$ MPa, and it corresponds to the strain $\Delta l/l$. Because the direction of the magnetic moments was turned to that of the current (i.e., longitudinal direction in Fig. 1) when the compressive stress σ was applied, the resistance was increased. In addition, a gauge factor (*GF*), i.e., the sensitivity, which is defined as $(\Delta\rho/\rho) \times (\Delta l/l)$, was estimated to be about 1.9. Its value is about 13 times larger than the GF in a metallic wire electrical-resistance strain gauge (Kyowa Electronic Instruments; KFR-1–120-C1-16).

On the other hand, the change in resistivity $\Delta\rho/\rho$ was saturated when compressive stress σ reached value in excess of 50 MPa, implying that the magnetic moments in the magnetic film were turned to the longitudinal direction in Fig. 1 completely. Under such conditions a hysteresis loop has disappeared.

Figure 6 shows a relation between GF in the linear response range, static susceptibility χ_{h0}, and Ni–Fe layer thickness t_F in the strain sensor with Mn–Ir (10 nm)/Ni–Fe (t_F nm)/Ru (1 nm) exchange-coupled film. In Fig. 6, when increasing Ni–Fe layer thickness t_F in the strain sensor, both the GF and the static susceptibility χ_{h0} increased. The result of the static susceptibility χ_{h0} agrees with Eq. (2).

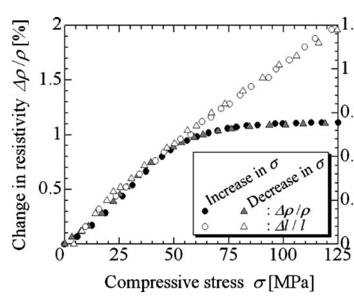

FIG. 5. Relation between change in resistivity $\Delta\rho/\rho$, strain $\Delta l/l$, and compressive stress σ in the strain sensor with Mn–Ir (10 nm)/Ni–Fe (50 nm)/Ru (1 nm) exchange-coupled film.

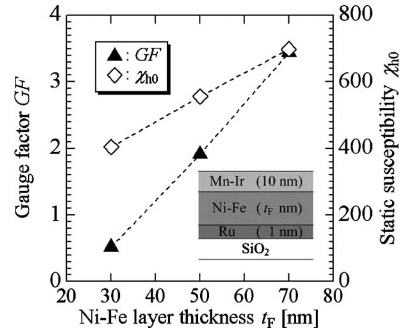

FIG. 6. Relation between GF, static susceptibility χ_{h0}, and Ni–Fe layer thickness t_F in the strain sensor with Mn–Ir (10 nm)/Ni–Fe (t_F nm)/Ru (1 nm) exchange-coupled film.

V. CONCLUSION

The strain sensors using stress-MR effect of Mn–Ir/Ni–Fe/Ru exchange-coupled magnetic film were fabricated and investigated. The results are obtained as follows.

(1) The exchange bias field H_{ex} is nearly inversely proportional to the Ni–Fe layer thickness t_F in the Mn–Ir/Ni–Fe/Ru exchange-coupled film. The exchange energy J_{ex} of the Mn–Ir/Ni–Fe interface was estimated to be $0.043\ \text{erg/cm}^2$.

(2) The angle θ of the easy axis in the magnetic film and longitudinal direction was estimated to be about 46° because of pinning field for the exchange-coupled film.

(3) The change in resistivity $\Delta\rho/\rho$ is proportional to the applied compressive stress σ for $\sigma \leqq 50$ MPa in the strain sensors with Mn–Ir(10 nm)/Ni–Fe (50 nm)/Ru (1 nm) exchange-coupled magnetic film. The GF is about 1.9 which is 13 times larger than that of a metallic wire electrical-resistance strain gauge. Moreover a hysteresis loop disappeared.

(4) When increasing Ni–Fe layer thickness t_F in the strain sensor with Mn–Ir/Ni–Fe/Ru exchange-coupled magnetic film, both the GF and the static susceptibility χ_{h0} increased.

[1]M. Nishibu, Y. Okada, K. Sakamoto, T. Sato, K. Yamasawa, and Y. Miura, The 2006 Annual Meeting Record of IEE Japan, 2006 (unpublished), Paper No. MAG-02-139, pp. 155–156.
[2]S. Chikazumi, K. Ohta, K. Adachi, N. Tsuya, and Y. Ishikawa, *Jiseitai Handbook*, (Asakura Shoten, Tokyo, 1975), p. 832.
[3]K. Kakuno, J. Magn. Soc. Jpn **26**, 5 (2002).
[4]Y. Okada, M. Nishibu, K. Sakamoto, T. Sato, K. Yamasawa, and Y. Miura, J. Magn. Soc. Jpn **31**, 356 (2007).
[5]M. Jimbo, J. Magn. Soc. Jpn **22**, 12 (1988).
[6]M. Sonehara, T. Sato, K. Yamasawa, Y. Miura, and M. Yamaguchi, Trans. Mater. Res. Soc. Jpn. **29**, 1735 (2004).
[7]M. Sonehara, T. Sugiyama, T. Sato, K. Yamasawa, and Y. Miura, IEEE Trans. Magn. **41**, 3511 (2005).
[8]M. Sonehara, T. Sugiyama, T. Ishikawa, T. Sato, K. Yamasawa, and Y. Miura, IEEE Trans. Magn. **42**, 2984 (2006).